Kinetics of spontaneous microgels adsorption and stabilization of emulsions produced using microfluidics

Marie Charlotte Tatry, Eric Laurichesse, Adeline Perro, Valérie Ravaine, Véronique Schmitt

Kinetics of spontaneous microgels adsorption and stabilization of emulsions produced using microfluidics

Marie Charlotte Tatry[1,2], Eric Laurichesse[1], Adeline Perro[2], Valérie Ravaine[2*] and Véronique Schmitt[1*]

[1] Centre de Recherche Paul Pascal, UMR 5031, Université de Bordeaux, CNRS, 115 Avenue du Dr A. Schweitzer, 33600 Pessac, France.

[2] Université de Bordeaux, ISM, CNRS UMR 5255, Bordeaux INP, Site ENSCBP, 16 Avenue Pey Berland, 33607 Pessac Cedex, France.

* corresponding authors
Email: schmitt@crpp-bordeaux.cnrs.fr
Email: vravaine@enscbp.fr

KEYWORDS

Microgels

Interfaces

Adsorption

Kinetics

Spontaneous adsorption

Emulsions

Microfluidic emulsions

ABBREVIATIONS

pNIPAM	poly(N-isopropylacrylamide)
pNIPAM-AA	poly(N-isopropylacrylamide) containing acrylic acid
BIS	N,N′-methylenebis(acrylamide)
KPS	potassium persulfate
LCST	Lower Critical Solution Temperature
VPTT	Volume Phase Transition Temperature
SANS	Small Angle Neutrons Scattering

TEM	Transmission Electronic Microscopy
SEM	Scanning Electronic Microscopy
PDI	PolyDispersity Index

Abstract

The aim of the paper is to examine the adsorption kinetics of soft microgels and to understand the role of fundamental parameters such as electrostatics and deformability on the process. This knowledge is further exploited to produce microgel-stabilized emulsions using a co-flow microfluidic device.

Uncharged microgels made of poly(N-isopropylacrylamide) are synthesized with variable cross-linker contents, and charged ones are produced by introducing pH sensitive co-monomers during the synthesis. The study is carried out by measuring the microgels adsorption kinetics by means of the pendant drop method. The surface pressure is derived from the previous results as a function of time and is measured as a function of the area compression using a Langmuir trough. Emulsions are produced using a microfluidic device varying the microgels concentration and their stability is visually assessed.

The microgels deformability as well as higher particle concentration favour their adsorption. The adsorption is not governed by diffusion, it is cooperative and irreversible. Conversely, the kinetics is slowed down for increasing cross-linking density. The presence of charges slows down the kinetics of adsorption. In the presence of electrolyte, the kinetics accelerates and becomes similar to the one of neutral microgels. The original features of microgel adsorption is highlighted and the differences with adsorption of polymers, star polymers, proteins, and polyelectrolytes are emphasized. Taking benefit from the adsorption kinetics, the required formulation conditions for producing microgel-stabilized emulsions using a co-flow microfluidic device are derived.

There exists a critical concentration above which microgels spontaneously adsorb in a sufficient way to decrease the interfacial tension. This critical microgel concentration increases with the cross-linking density and is higher for charged microgels. Whatever the kinetics, the same surface pressure is finally reached. This peculiar behaviour is likely a consequence of the

presence of dangling chains in the as-prepared microgels. Consequently, a microgel excess is required to produce emulsions using microfluidics where adsorption has to be spontaneous.

Graphical abstract

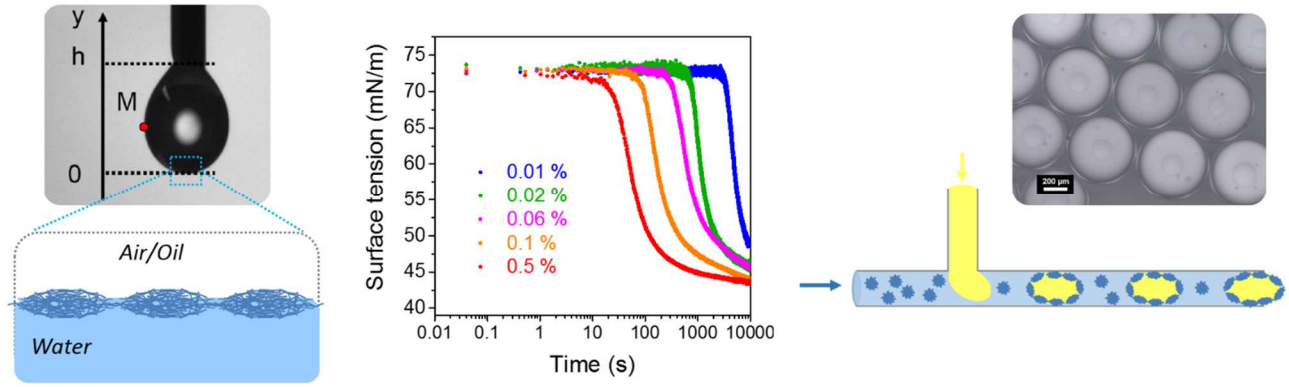

1) Introduction

Microgels are soft and deformable particles containing low amount of cross-linkers [1-5]. Such particles are highly swollen by the solvent. The most studied microgels are probably microgels made of poly(*N*-isopropylacrylamide) noted hereafter (pNIPAM) [1]. Since this polymer exhibits a Lower Critical Solution Temperature (LCST), the microgels are sensitive to temperature: at room temperature, due to the amide function, hydrogen bonds are formed and the microgels are swollen by water, whereas when the temperature is raised above the so-called volume phase transition temperature (VPTT), the hydrogen bonds break and the microgels contract. Depending on the cross-linking rate, the swelling ratio (swollen microgel volume to collapsed microgel volume ratio) can reach high values: above 10 [5,6]. Due to the small microgel size (10-1000 nm), the volume change operates quickly. In a batch precipitation process, the structure of the microgels is highly dependent on their synthesis and the cross-linker reactivity compared to the major monomer's one. Using N,N′-methylenebis(acrylamide) (BIS) as a cross-linker, which reacts faster than NIPAM [7], yields microgels with a radial gradient of cross-linking density from the center to the periphery, as confirmed by Richtering and co-workers by SANS [8,9]. The obtained microgels can then be represented as a quite hard core surrounded by a shell composed of dangling chains visible using TEM [10]. On the contrary, when the cross-linker is gradually added during the synthesis to compensate the reactivity mismatch, the monomer and cross-linker distributions in microgels are more even [11,12]. The most studied microgels are prepared by batch polymerization. It has been earlier demonstrated that such microgels are able to adsorb spontaneously at any temperature [13-16] giving rise to a sensible decrease of the interfacial tension. It is also known that such microgels are able to stabilize emulsions [17-20]. In a previous paper, we demonstrated the importance of microgels deformability on the ability to stabilize emulsion and on the way microgels pack at drop surfaces [10]. The deformability as well as the uneven distribution of the cross-linker have

also consequences on many emulsions features like emulsion flocculation state, emulsion resistance to handling [10,21] … Additionally to the temperature sensitivity, a pH-sensitivity can be conferred to the microgels by introducing a pH sensitive monomer [10,19,22,23] as for example an acidic function during the synthesis. Again, depending on the monomer reactivity, the charges can be distributed homogeneously in the microgels or preferentially at the periphery [23-25]. Such charged microgels are also able to stabilize emulsions that become temperature and pH-sensitive [10,19,22,23].

Although the microgels abilities to adsorb at an interface and to stabilize emulsions are known, many questions remain about *i*) the reversibility of the microgel adsorption, *ii*) the role of impurities (arising from the synthesis) on the microgels adsorption and *iii*) the role of charges coming from the monomer on the adsorption kinetics. It is also of high importance to determine the major parameters influencing the adsorption kinetics. In order to bring more understanding in the microgels kinetics, in the present paper, we investigate these features at the air-water and oil-water interfaces at room temperature and we propose a direct link between the adsorption kinetics and the conditions required to produce microgel-stabilized emulsions using co-flow microfluidics.

2) Materials and methods

2.1. Chemicals

All reagents were purchased from Sigma-Aldrich. *N*-isopropylacrylamide (NIPAM) was recrystallized from hexane (ICS) and dried under vacuum overnight prior to use. *N,N'*-methylenebis(acrylamide) (BIS), acrylic acid (AA), potassium persulfate (KPS) for the synthesis and n-dodecane (purity >99%) for interfacial tension measurements were used as received. Milli-Q water was used for all synthesis reactions, purification, and solution preparation.

2.2. Particles synthesis and purification

pNIPAM microgels bearing different charges were synthesized. We synthesised “quasi-neutral” pNIPAM microgels at different cross-linking densities (1.5, 2.5 and 5 mol% respectively) keeping their diameter at 25°C approximately constant of the order of 650 nm. “Quasi-neutral” pNIPAM microgels were obtained by copolymerization of NIPAM and BIS, the term “quasi neutral” refers to the fact that very low amounts of charges could be brought by the initiation step. “Charged” microgels, noted pNIPAM-AA in the following, resulted from the copolymerization of NIPAM, BIS and acrylic acid (10 mol%). The presence of carboxylic groups introduces additional charges when the pH is above the pKa of the acrylic acid (pKa=4.5). The cross-linker concentration was kept constant and equal to 2.5 mol% with respect to NIPAM. According to previous work by Pelton *et al*. [24] , pNIPAM-AA exhibit relatively low block content and a relatively homogeneous radial distribution of the charges in the gel matrix.

The microgels were obtained by an aqueous free-radical precipitation polymerization classically employed for the synthesis of thermo-responsive microgels and especially pNIPAM microgels [1,7]. Polymerization was performed in a 500 mL three-neck round-bottom flask, equipped with a magnetic stir bar, a reflux condenser, thermometer, and argon inlet. NIPAM and BIS were dissolved in 290 mL of water. The solutions were purified through a 0.2 µm membrane filter to remove residual particulate matter. The solutions were then heated up to 70°C with argon thoroughly bubbling during at least 1 hour prior to initiation. For “charged” microgels, an appropriate amount of acrylic acid comonomer AA was introduced. The initial total monomer concentration was held constant at 70 mM. The content of BIS was usually equal to 2.5 mol% compared to NIPAM, unless otherwise noted. Free radical polymerization was then initiated with KPS (2.5 mM) dissolved in 10 mL of water after 10 min of argon degassing. The initially transparent solutions became progressively turbid as a consequence of the

polymerization and precipitation process. The solutions were allowed to react for a period of 6 hours in the presence of argon under stirring. After this period of time, a homogeneous suspension was obtained.

To eliminate possible chemical residues, the microgels were purified by centrifugation-redispersion cycles at least five times (16 000 tr.min^{-1} corresponding to 29 220 g_r where g_r is the terrestrial acceleration, for 1 hour, at 24°C). Each centrifugation allowed phase separating the sample between a white liquid appearing homogeneous in the bottom containing the microgels and a transparent liquid on the top, called supernatant and noted S_i, where i varies from 1 to 6. Each supernatant was removed and its surface tension was measured by the pendant drop method. Apart from the experiments performed for the dedicated study (described in section 3.1), the purification was repeated until the surface tension of the supernatant reached a value close to the one of pure water, *i.e.* above 72.8 mN/m (on a 50 seconds period of time) showing that the microgel dispersions were almost free of surface active impurities.

The charge content of these microgels has been derived previously from the mobility measurements using Ohshima's model [26]. For the same pNIPAM and pNIPAM-AA microgels, the content of charge in the polymer was 0.05 and 3.97 mol% respectively at pH 6, so that the former will be called neutral and the last charged [23].

The particle mass m_{part} (in wt%) in aqueous dispersions was determined by the drying method. A known amount of the dispersion was dried above 50°C and then weighted. Following Lele *et al.*, this mass is composed of 29% of polymer and 71% of water [27]. In the following, the concentration of microgels is expressed in terms of m_{part} in the suspension.

2.3. Particle size characterization

Particle sizes and polydispersity index were determined by dynamic light scattering (DLS) with a Zetasizer Nano S90 Malvern Instruments equipped with a HeNe laser at 90°. Hydrodynamic diameters were calculated from diffusion coefficient using the Stokes-Einstein

equation. All correlogram analyses were performed with the software supplied by the manufacturer. The polydispersity index (PDI) is given by the cumulant analysis method. The obtained results are the following (Table 1).

Table 1: Main characteristic of the synthesized microgels

mol% of BIS		**Hydrodynamic diameter (nm)**		**Polydispersity index (PDI)**	
Neutral microgels pNIPAM	Charged microgels pNIPAM-AA	T<VPTT 25°C	T>VPTT 50°C	T<VPTT 25°C	T>VPTT 50°C
1.5	/	668	295	0.085	0.137
2.5	/	620	273	0.012	0.173
5	/	633	358	0.042	0.152
/	2.5	1020	472	0.046	0.287

2.4. Dynamic surface tension

We determined dynamic interfacial tension of the air/water and oil/water interfaces using the pendant-drop technique (Teclis). An aqueous drop containing a known concentration of microgels was suspended in air or immersed in the oil. A drop of 10 µL was created, corresponding to a drop surface area of approximately 22 mm² in order to ensure an excess of particles compared to the amount of interface ($n_{particles}$=1.12 10^8). The tension was deduced from the axisymmetric drop shape by fitting with the Laplace equation. A constant drop volume was maintained over 10 000 seconds and the tension was recorded as a function of time. In this method, the microgels spontaneous adsorption at the interface was assessed.

2.5. Microfluidic device

The formation of drops stabilized by microgels was performed by exploiting a co-flow microfluidic device. The system consisted of two coaxial capillaries connected with a T-junction (UpChurch Scientific, 1/16). This T-junction allowed the alignment of the two

capillaries favoring the injection of the dispersed phase into the continuous medium. The inner capillary was a surface modified fused silica tube (inside diameter (ID) 75 µm; outside diameter (OD) 148 µm; Polymicro technologies). The surface modification, which increased the hydrophobicity of the capillary, was performed following an approach described previously [28]. The external capillary was a silica tube of at least 10 cm in length (ID, 455 µm; OD 670 µm; Polymicro technologies).

An aqueous solution of microgels (0.1-1 wt%) was used as the continuous phase. The influence of salt was analyzed by adding up to 0.01 M of NaCl. The dispersed phase was dodecane. The flow rates were fixed at 0.1 $mL.h^{-1}$ and 0.4 $mL.h^{-1}$ for the inner and outer solution, respectively. In such conditions, the characteristic time for the droplet formation is in the order of magnitude of the second and the residence time of one minute.

2.6. Cryo-SEM observations

Cryo-SEM observations were carried out with a JEOL 6700FEG electron microscope equipped with liquid nitrogen cooled sample preparation and transfer units. A drop of emulsion was first set on the aluminum specimen holder. The sample was frozen in the slushing station with boiling liquid nitrogen. The specimen was transferred under vacuum from the slushing station to the preparation chamber. The latter was held at T=-150°C and was equipped with a blade used to fracture the sample. In case of sublimation, the temperature in the preparation chamber was raised to -50°C for less than 5 min before decreasing the temperature again.

3) Results

3.1. Role of impurities on the adsorption kinetics surface tension

The kinetics of adsorption at the air/water interface of the successive supernatants noted S_i with i varying from 2 to 6 (see Materials and Methods §) has been studied. The results are

reported in Fig. 1a. The two first supernatants exhibit a very fast surface tension decrease reaching almost immediately a value close to 45 mN/m showing the presence of synthesis residues able to spontaneously adsorb at the interface. These residues are likely monomers and/or oligomers. Depending on the sampling, non-sedimented microgels could also be present in the first supernatants. This is unlikely the case for the further supernatants.

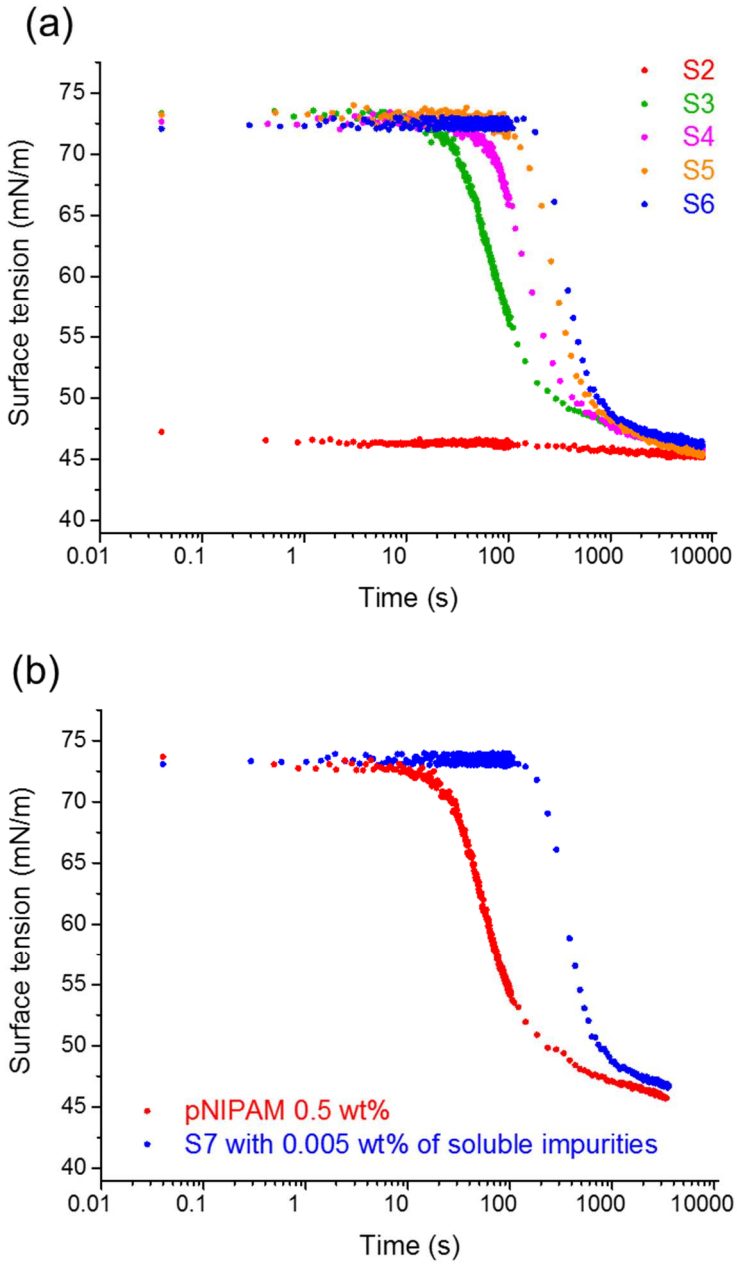

Figure 1: Surface properties of the various supernatants (a) kinetics of adsorption (S2: red, S3: green, S4: pink, S5: orange, S6: blue) and (b) comparison with cleaned microgels (5 cleaning steps), see text for more explanation.

In order to further investigate the role and amount of these impurities, we estimated the amount of residual solid in the supernatant by weighting the dried mass of a known amount of supernatant. The results, listed in Table 2, show the efficiency of the various cleaning steps.

Table 2: Proportion of solid content in the supernatants expressed in wt% with respect to the amount of supernatant.

S1	**S2**	**S3**	**S4**	**S5**	**S6**
Just after synthesis	After 1st washing	After 2nd washing	After 3rd washing	After 4th washing	After 5th washing
0.26	0.04	0.025	0.021	0.012	0.01

For the supernatants, the amount of residues decreases and the kinetics of adsorption slows down noticeably even more since the number of washing cycle increases. After 5 cycles, in the sixth supernatant, the residues represents 0.01 wt% of the aqueous phase (corresponding to 0.87 wt% with respect to the total polymer content while microgels represent 99.13 wt%). After removing the sixth supernatant, we analysed the sediment. For this purpose, a known amount of water was added, the sample was homogenized and a new centrifugation step was operated allowing separating the soluble part (S_7) and the sediment. The solid contents of the two sample parts were determined. The composition of the 6th sediment could therefore be assessed: the soluble part represented 1% of the sedimented microgels meaning that if a microgel suspension is prepared from the 6th sediment to reach for example 0.5 wt% of microgels, it also contains 0.005 wt% of the soluble impurities. To determine the impact of these impurities on the kinetics

of adsorption, a solution containing 0.005 wt% of the soluble impurities was prepared using the 7th supernatant and compared to a suspension composed of 0.5 wt% of the sixth sediment. The results are reported on Fig. 1b. It can be observed that the impurities remaining after 5 washing cycles adsorbed to the interface with a much larger characteristic time. The process is approximately 6 times slower. It is worth noticing that the final value is the same. We will discuss this point later. From these experiments, it can be concluded that washing the microgels is crucial for adsorption studies and that after 5 washing steps, a small amount of soluble species remains in the suspension. These latter adsorbed much slower than the microgels themselves so that the residual impurities after 5 washing steps do not affect anymore their adsorption. Therefore, in the rest of the study, all the microgels have been washed 5 times.

3.2. Role of neutral microgel concentration

The kinetics of adsorption have been measured both at the air/water (Fig. 2) and the dodecane/water (see Supporting Info SI.1) interfaces for the microgels synthesised with 2.5 mol% of cross-linker. The adsorption kinetics are similar, the difference resides in the interfacial tension values because of the different interfacial tensions of air/water and oil/water. Also, the pressures are a little different likely due to the possible presence of unwanted compounds of amphiphilic character as proposed in Ref. [29]. The observed similarity between the two interfaces means that the adsorption phenomenon is similar. In the following unless otherwise specified, the results are reported for the air/water interface to avoid the presence of such compounds. The measurements were performed in presence of NaCl at 10^{-4} M in order to fix the ionic strength to a low value making the dispersion insensitive to external impurities but without efficient screening effect (Debye length κ^{-1}=30 nm).

The surface tension measurements $\gamma(t)$ or equivalently the deduced surface pressure defined as $\pi(t)=\gamma_0-\gamma(t)$ where γ_0 is the pristine interfacial tension equal here to 72.8 mN/m (air/water interface) are plotted on Supporting Information SI.2 and Fig.2 (a) and (b) respectively.

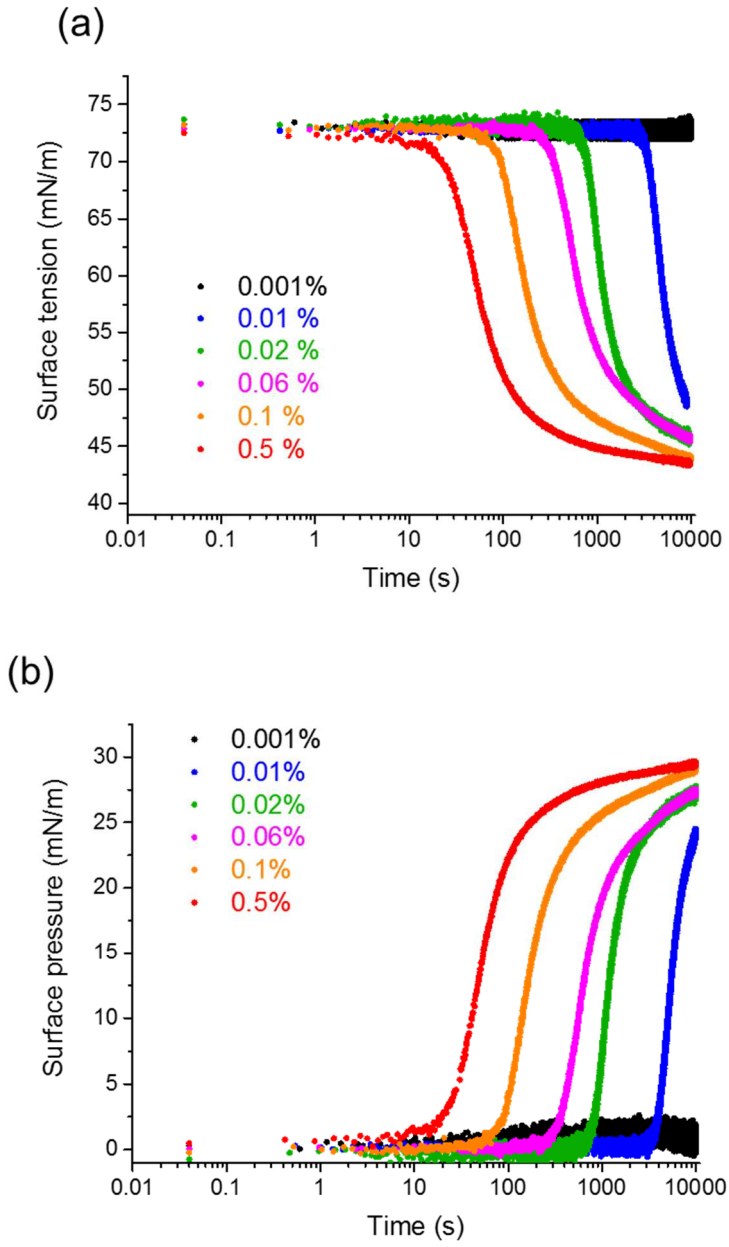

Figure 2: Influence of the microgels concentration on (a) the surface tension and (b) deduced spontaneous surface pressure for pNIPAM microgels with a fixed cross-linking density (BIS 2.5 mol%) in presence of NaCl at 10^{-4} M.

From Fig. 2, it can be seen that adsorption becomes significant above a critical threshold (>0.001%) in the considered 10 000 s period of time (corresponding to a little more than 2 hours and 45 minutes). Moreover, the kinetics is faster as the concentration increases reaching in all cases the same plateau value γ_f.

3.3. Role of added salt to neutral microgels

The same experiments were carried out in presence of NaCl 10^{-2} M. At such a concentration, the microgels remain dispersed in the suspension and their size is unchanged [23]. The estimated Debye length κ^{-1} is equal to 3 nm. The results are reported in Fig. 3.

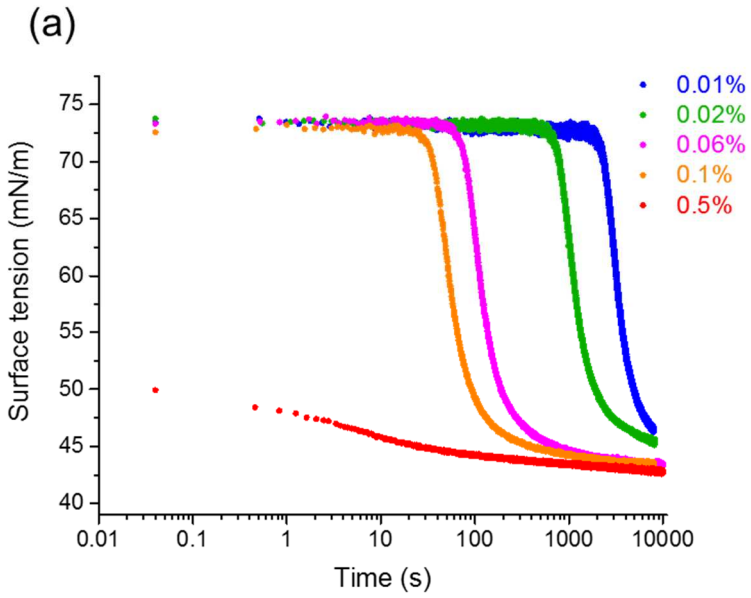

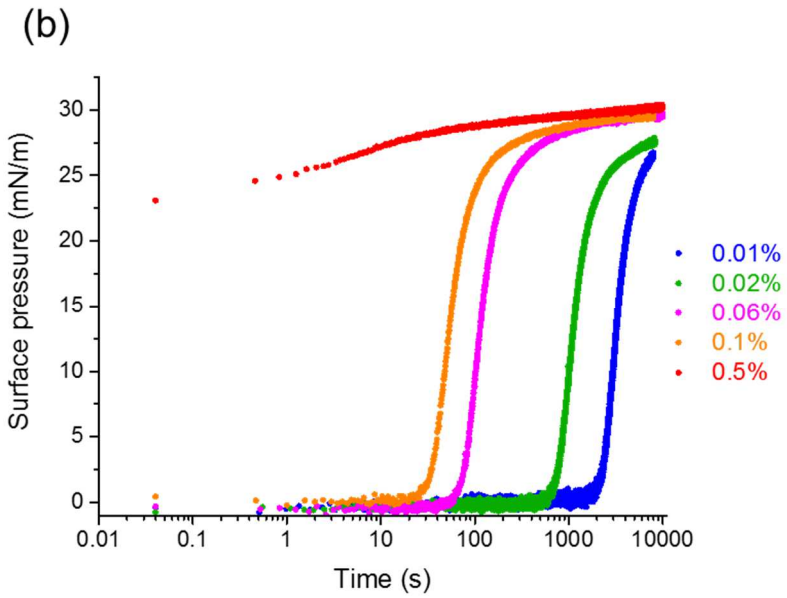

Figure 3: Influence of the microgels concentration on (a) the surface tension and (b) deduced spontaneous surface pressure for pNIPAM microgels with a fixed cross-linking density (BIS 2.5 mol%) in presence of NaCl at 10^{-2} M.

The main trends are the same as previously noted. All the curves converge towards the same pressure with a faster kinetics as the microgel concentration increases. It can also been noted that the addition of salt seems to slightly accelerate the kinetics even if the microgels can be considered as uncharged. Indeed, before the cleaning cycles, they possess a very low charge density (0.05 mol%) arising from the initiation step [23].

3.4. Role of the microgel deformability

By varying the cross-linker concentration during the synthesis, the microgel deformability was varied as in Ref. [10]. To assess the effect of this parameter, we fixed the microgel concentration to 0.1 wt%. The results are reported in Fig.4 for the surface pressure and in Supporting Information SI.3 for the measured surface tension.

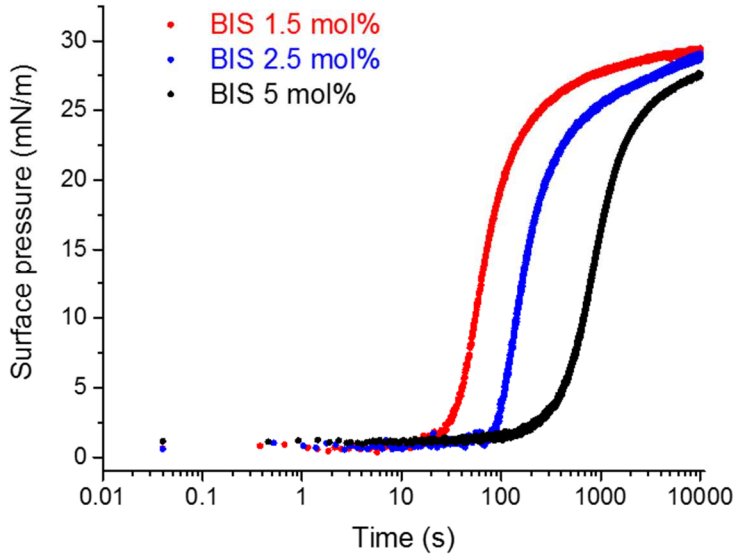

Figure 4: Influence of the cross-linking density on the spontaneous surface pressure. The microgel concentration is kept constant $C_{microgels}$= 0.1 wt% and the cross-linking density is varied through the BIS content: 1.5 mol% (red), 2.5 mol% (blue) and 5 mol% (black), in presence of NaCl at 10^{-4} M.

As can be observed from Fig.4, all the microgels adsorb spontaneously and reach the same final pressure. The adsorption kinetics is faster for more deformable microgels. This is likely linked to the core-shell structure of microgels (bearing numerous dangling chains) leading to a faster adsorption of amphiphilic moieties.

Note that the adsorption of rigid homogeneous solid non interacting particles would lead to an unmeasurable decrease of the surface tension *i.e.* a zero surface pressure using Langmuir compression until particles were in contact and steric repulsion [30] was experienced. Such a low osmotic pressure is the result of the large particle size and consequently to the very low surface density. A rough estimate of the corresponding 2D surface pressure of spherical objects having the same size (700 nm in diameter) as the microgels would give 10^{-8} N/m.

3.5. Role of the charges in pNIPAM-AA microgels

During the synthesis, 10 mol% of acrylic acid was incorporated in the microgels containing 2.5 mol% of cross-linker. According to previous studies [24,25], the radial distribution of the charges is relatively homogeneous. As the pKa of acrylic acid is 4.25, in distilled water (pH=6) the ionisation may be considered as total. The effect of the microgels concentration was measured in presence of 10^{-4} M and 10^{-2} M of NaCl. The results are reported in Fig. 5 (a) and (b) respectively.

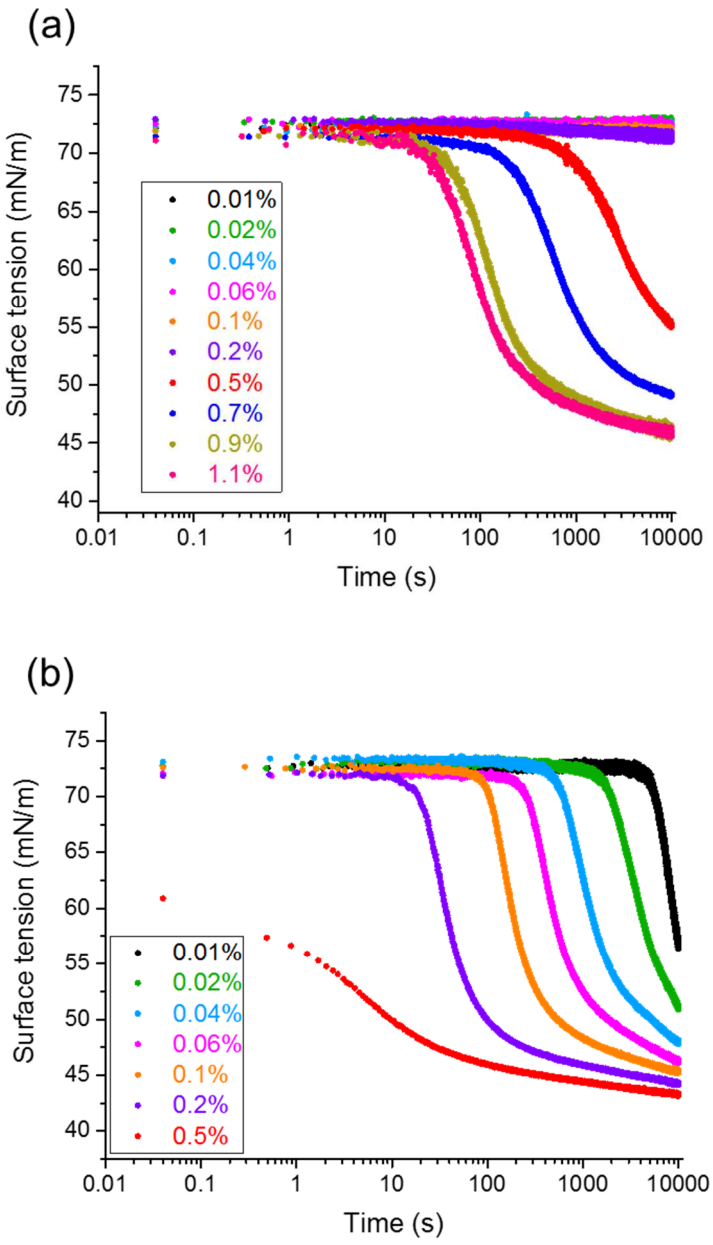

Figure 5: Influence of concentration and salt on the pNIPAM-AA microgels adsorption kinetics (a) 10^{-4} M of NaCl and (b) and 10^{-2} M.

From Fig. 5a, it appears that charged microgels also exhibit a threshold concentration below which no decrease of surface tension could be detected over 10 000 seconds. This threshold value is approximately 0.3 wt% a value much higher (300 fold) than the one determined for neutral microgels (0.001 wt%). Moreover, it can be noticed that the kinetics are much slower than for neutral pNIPAM microgels. When salt is added, even the lowest studied concentration of pNIPAM-AA microgels leads to a high decrease of the surface tension and the kinetics of adsorption are speeded up compared to the ones measured for charged microgels.

3.6. Emulsion production using a co-flow microfluidic device

The aim was to determine the effects of microgels concentration and presence of charges on the possibility to produce emulsions using a co-flow microfluidic device. For this purpose, the process parameters (flow rates of continuous and dispersed oil phase) were kept constant, only the formulation parameters (type and concentration of microgels, presence of salt) were modified. We observed that drops produced at low microgels concentration immediately coalesced ($t<1s$) after leaving the capillary (or after being expelled from the capillary). Conversely, above a threshold concentration, the produced drops accumulated at the top of the collecting vessel. Although mechanically fragile, they remained stable at rest for several months. It can be noticed that the produced emulsions were not flocculated at all; the drops were not bridged contrarily to emulsions produced upon high shear rate [18]. Instead, using microfluidics, the drops were well dispersed and move freely with respect to each other. The limit concentrations above which emulsion could be produced are reported in Fig.6.

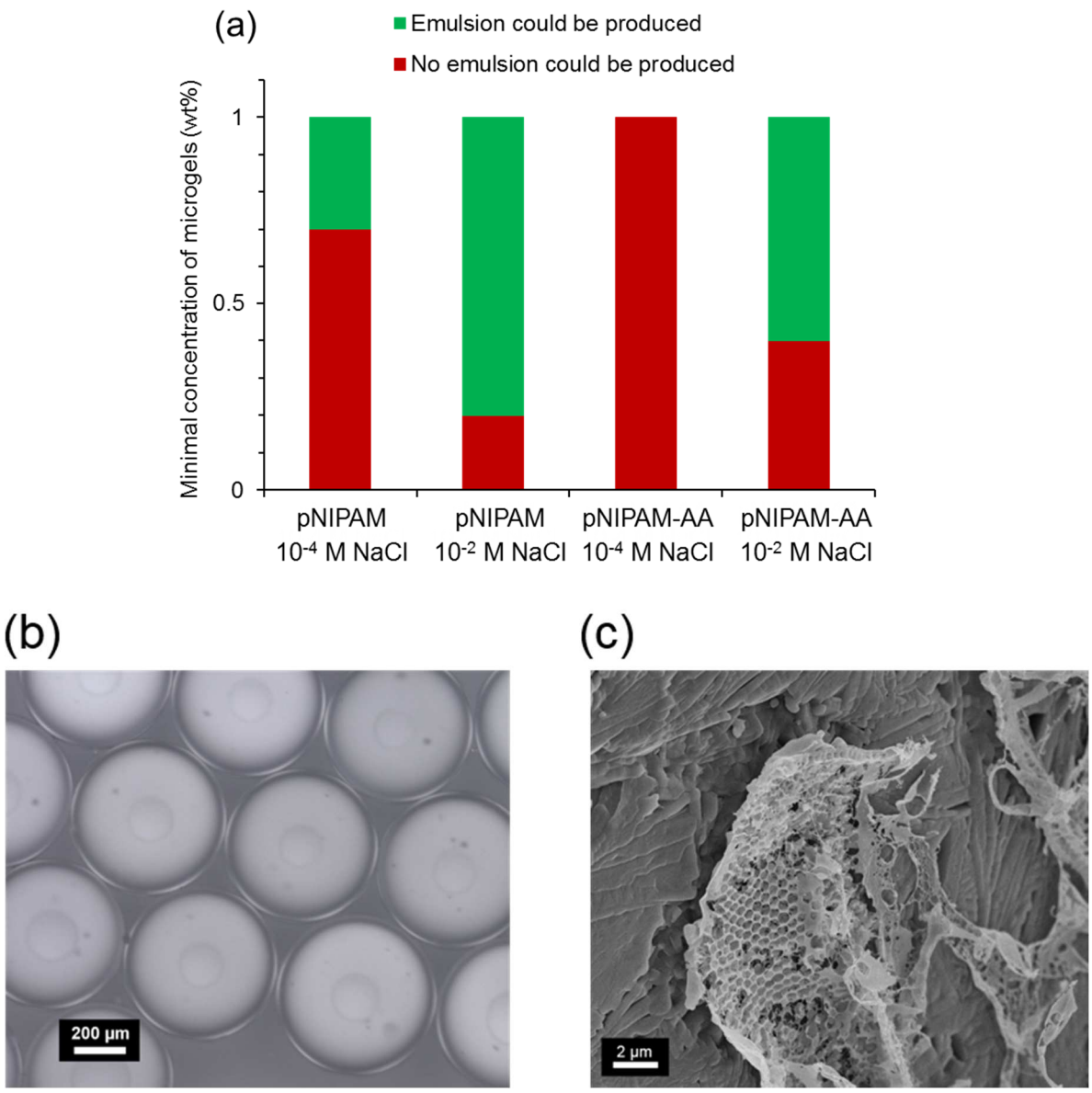

Figure 6: (a) Minimal microgel concentration required to produce stable drops using our microfluidic device. (b) Example of an emulsion obtained with the microfluidic device using 0.6 wt% of pNIPAM-AA with 0.1 M of NaCl. (c) CryoSEM picture obtained on an emulsion stabilized by 0.56 wt% of pNIPAM microgels with 0.05 M of NaCl.

It is interesting to notice the effect of added salt. Indeed, for charged microgels, no emulsion could be obtained up to 1 wt% while adding salt reduces the minimal microgels concentration required to stabilize the drops. These observations are in qualitative agreement with the adsorption kinetics. A centre-to-centre distance of 460 ± 40 nm can be deduced from such

pictures. This distance can be compared to their hydrodynamic diameter measured at 25°C by DLS in the suspension (700 nm).

4) Discussion

4.1 Irreversibility of the adsorption

Microgels spontaneously adsorb at the air/water or oil/water interface. To determine the excess surface Γ and the coverage rate θ, all the classical models (Langmuir, Frumkin…) presuppose the reversibility of the adsorption. In order to determine whether the adsorption is reversible or not, we performed the following test using the pendent drop device. An air bubble is formed at the tip of the syringe immersed in a water phase containing pNIPAM microgels at 0.01 wt% containing 2.5 mol% of cross-linker. Once the surface tension equilibrated at approximately 45 mN/m (the same value as the one obtained with a drop of microgel dispersion in air), the external phase is diluted with pure water and very carefully replaced by pure water to avoid bubble detachment. In case of an adsorption equilibrium, the interfacial tension is expected to increase as a signature of microgel desorption. No increase of the interfacial tension could be detected over a period of about 1000 seconds showing that the adsorption is irreversible. This result is in agreement with observations made previously on the oil/water interface [31]. As a consequence, isotherm equations cannot be used and the surface excess Γ cannot be determined reliably.

4.2 Adsorption characteristics

All the adsorption curves exhibit the same shape with a decrease from the initial to a final value γ_f at 10 000 s. The high surface pressure instantaneously reached by these soft particles is very different from hard spheres of equivalent size used as Pickering stabilizers. Indeed, in this last case, due to the large particle size and hence low surface density, no surface tension evolution can be detected. Moreover, in the present case, soluble moieties adsorb and reach the

same value (Fig. 1b). One can conclude that the surface tension reduction is due to the adsorption of microgel "fragments". More precisely, even if pNIPAM microgels are highly hydrophilic and swollen by solvent, they contain a large amounts of more lipophilic isopropyl functions likely able to adsorb. We think that the accessibility of these groups to the interface is due to the existence of dangling chains that have high mobility compared to cross-linked "blocked" chains.

Neutral microgels

Increasing the concentration or the microgels deformability accelerates the adsorption kinetics but does not influence the final value, meaning that whatever the concentration, the density of adsorbable moieties is enough to saturate the surface.

The shape of the curve can be compared to those obtained for proteins [32,33]. Two features are common: the time lag (time before the tension begins to decrease) that we observed most often except for very high microgel concentrations also called induction time and the occurrence of a minimal microgel concentration to get a tension decrease. These two features were thought to characterize a critical surface coverage, the induction time corresponding to the time needed for the protein surface concentration to reach this critical value. Below this critical surface coverage value, the surface pressure is negligible. Some differences can also be noted between microgels and proteins: for microgels, the surface pressure remains constant after the strong increase while for protein, due to denaturation that continuously happens [33-36], the pressure continuously increases with a small slope and no true equilibrium state can be established. Another important difference lies in the final value that does not depend on the microgels concentration while a concentration dependence is observed for proteins [36,37].

We can therefore conclude that microgels do neither behave like particles nor like proteins. However, it seems that, like for proteins, adsorption is linked to the presence of localized moieties and that the surface tension decreases only if enough of these moieties adsorb leading

to an increase of the surface pressure. Unlike denaturation of proteins, the conformation of microgels does not evolve over more than 7 hours.

Some animal [38-41] or plant [42] proteins are also known to assemble into microgels in specific conditions (pH, Temperature, process…) and to stabilize emulsions or foams. Some natural cross-linker can also be added to enhance the microgels stability [43]. Few papers report their adsorption kinetics. It is worth noticing that for casein microgels γ_f depends on the casein concentrations [43] while the adsorption curves are completely superimposed for whey protein microgels [40] in the 0.05 to 0.35 wt% concentration range. Moreover, the reached surface pressures are usually weak, lower than 8 mN/m compared to 30 mN/m in the present case. Such differences are likely observed because adsorption is very sensitive to the microgels structure.

Adsorption of neutral microgels can be compared to star polymers [44]. Star PEO polymers confer higher surface pressures than the corresponding linear PEO polymer (same equivalent molar mass) and a higher concentration dependence. It is also worth noticing that no concentration-dependence has been observed over 3 decades in a limited concentration range for linear neutral polymers [45] as we observed for microgels.

Final adsorption state

The "final" value of the surface tension γ_f or equivalently of the surface pressure π_f are obviously defined when the microgel concentration is high enough so that a plateau value is reached. Due to differences in kinetics this is not always the case. For the sake of comparison and to avoid any ambiguity, we keep the same notation γ_f and π_f, that are now arbitrarily defined as the values obtained at 10 000 s even if we are aware that for such systems, these values are not the final ones but just an approximation of the final values. To allow better comparison, γ_f

and π_f are plotted as a function of microgel concentration for neutral and charged microgels in Supporting Information SI.4 and Fig. 7 respectively.

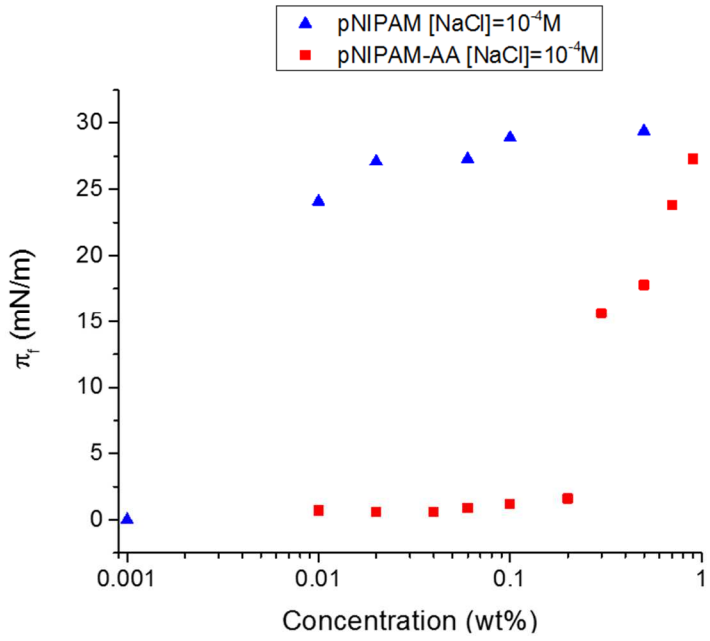

Figure 7: Evolution of the final spontaneous surface pressure π_f (at 10 000 s) as a function of the microgels concentration for "neutral" pNIPAM microgels (blue triangles) and charged pNIPAM-AA microgels (red squares) with [NaCl]=10^{-4} M.

The plots highlight the high critical concentration of 0.3 wt% of charged microgels before adsorption becomes detectable. Either no adsorption occurred or the lag time is larger than the experiment durations of 10 000 s. It seems that charged microgels hampered each other and inhibit the adsorption. Once the critical concentration (ca 1wt%) is overcome, the change is abrupt. It is worth noticing that at high microgel concentrations, the same spontaneous pressure is reached for neutral or charged microgels. At such high concentrations, a self-screening effect could occur. In order to test this hypothesis, one can estimate the amount of counterions present in the solution and the resulting Debye length. During the synthesis, 10 mol% of AA is added for charged microgels, taking into account the respective molar mass, this correspond to 8 mM of AA in a suspension of 1wt% of microgels. At pH 6 (larger than the considered pKa of AA

equal to 4.5), AA is ionized at 97% leading to a Debye length of 3.4 nm. As hypothesized, at 1wt% of charged microgels, the range of electrostatic repulsions has become short (of the same order than with 10^{-2} M of NaCl).

Such behaviour can be compared to the adsorption of strong polyelectrolytes [46-49]. Among them, the most studied one is sodium poly(styrenesulfonate) (PSS). Experiments performed on this latter show the existence of a critical concentration for observation of a surface pressure increase. The adsorption kinetics is much slower than for neutral polymers and it is generally attributed to the existence of an electrostatic adsorption barrier [47] as a result of strong repulsions between neighbouring charges. The surface tension evolves in two stages with a fast rate at short time and slow rate at long times. Only this first decrease is sensitive to salt (acceleration of the adsorption) in agreement with the explanation of reduction of the electrostatic barrier while the second stage is not affected showing a different mechanism. A widespread vision for the first stage is the following: adsorption is due to the compensation of electrostatic repulsion by high affinity between the polymer segments. As we did not assess adsorption at time larger than 10 000 s, we will not discuss the existence of a slow evolution of surface pressure at very large time scale and we only focus on the first stage. The charged microgels, like polyelectrolytes, exhibit a critical concentration before surface pressure increases and a strong acceleration when salt is added (Fig 5.b). However, in opposition to our observations, the surface pressure of the strong polyelectrolytes is dependent on the PSS concentration [47,48,50]. In the case of copolymers, the degree of hydrophobization of a polyelectrolyte main chain strongly influences the value of the critical concentration. For sodium 2-acrylamido-2-methyl-1-propansulfonate (AMPS) copolymerized with acrylamide (AM)(pAMPS-co-AM), this concentration is ca 0.1 wt% and thus close to the corresponding range for PSS, but for pAMPS-co-NIPAM that is to say with a more hydrophobic NIPAM monomer it is about 0.01 wt% and for the more hydrophilic poly(dimethyldiallylammonium

chloride) (PDMDAAC) it is of the order of 3 wt% [51]. This shows that this minimal concentration results from a balance between the electrostatic barrier towards adsorption and the degree of hydrophobicity. Even if the surface tension values are not directly discussed in [51], there are strong similarities with our observations.

Kinetics of adsorption

The characteristic time of adsorption t* is defined as the time required to decrease the surface tension by half of its final reduction rate or in other words for no experimental determination ambiguity the time required to reach a surface tension equal to 60 mN/m (or equivalently a pressure of 12 mN/m). Figure 8 reports t* as a function of microgel concentration for both neutral and charged microgels.

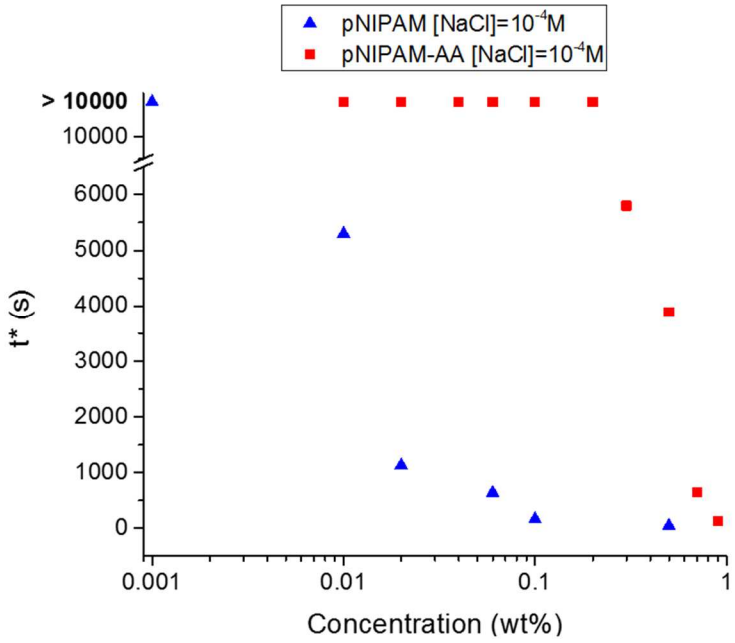

Figure 8: Evolution of the characteristic time t* (corresponding to the time for $\gamma \approx 60$ mN/m) as a function of the microgels concentration for neutral pNIPAM (blue triangles) microgels and charged pNIPAM-AA (red squares) microgels with [NaCl]=10^{-4} M.

Again, the figure makes very visible the need for a minimal microgel concentration. It also clearly evidences the huge difference in kinetics between neutral and charged microgels likely due to electrostatic repulsions as known for polyelectrolytes. The curves show a sharp evolution with microgel concentration above the critical concentration. From such an acceleration with microgel concentration, it can be deduced that the adsorption is not limited by the microgels diffusion. Only a cooperative phenomenon can explain it. This feature is very different from the one observed for proteins for which the diffusion governs the adsorption [36] as deduced from a square root variation of the adsorption time with the protein concentration. In fact in Ref. [36], the authors report the lag time not the adsorption time but this does not change the conclusion.

Effect of salt

The characteristic values of the adsorption curves: t*, γ_f and π_f are plotted in Fig. 9 as a function of microgel concentration for neutral and charged microgels at two ionic strengths.

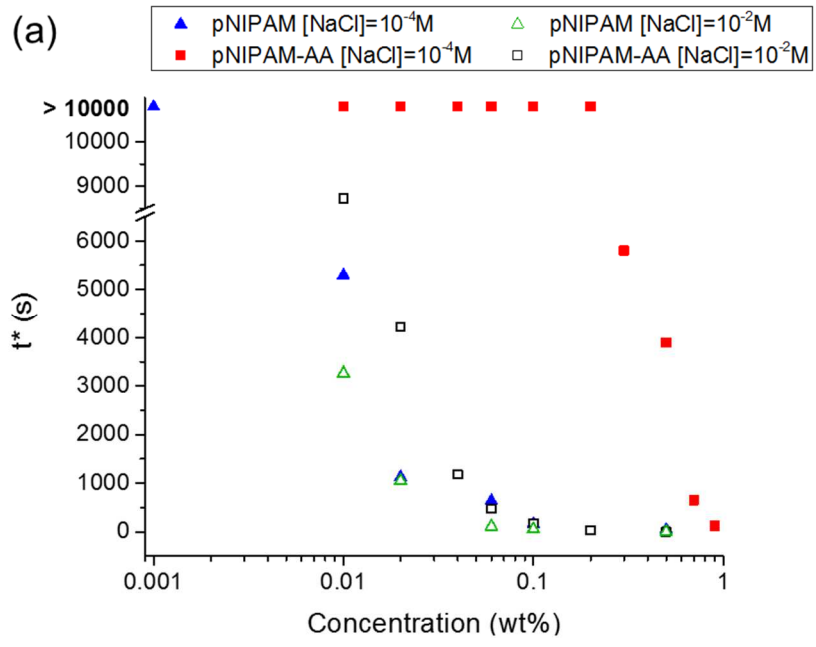

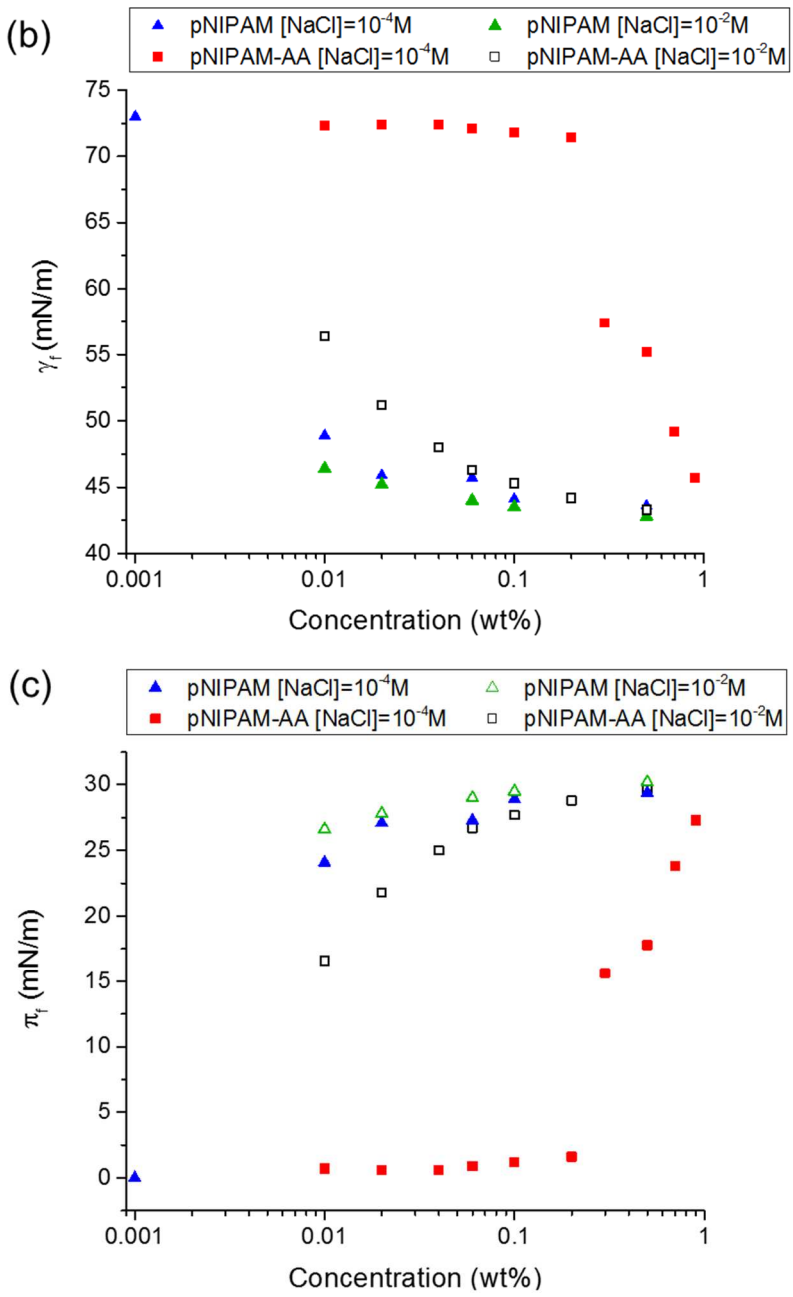

Figure 9: Comparison of the effect of salt and microgel concentration (a) on the adsorption kinetics assessed by t* and on the final state through (b) γ_f and (c) π_f for neutral and charged microgels. PNIPAM microgels with NaCl = 10^{-4} M (solid blue triangles), PNIPAM-AA microgels with NaCl = 10^{-4} M (solid red squares), PNIPAM microgels with NaCl = 10^{-2} M (open green triangles) and PNIPAM-AA microgels with NaCl = 10^{-2} M (open black squares).

As expected the presence of salt does almost not affect the adsorption of neutral microgels, a small acceleration of the kinetics at low concentration can be detected but this effect is very

moderate. Also it seems that the final pressure is slightly different for low concentration of microgels but it likely results from the fact that the plateau is not completely reached at 10 000 s and from the definition of γ_f. Conversely, the presence of salt considerably affects the adsorption of charged microgels especially at low concentrations. The values of t*, γ_f and π_f tend to converge towards those obtained for neutral microgels. It therefore seems that the charged PNIPAM-AA microgels behave as neutral PNIPAM microgels in presence of 10^{-2} M of NaCl (Debye length of 3 nm). This behaviour is close to the one observed for polyelectrolytes in presence of salt that shields the electrostatic repulsion at the origin of the adsorption barrier [51]. In order to better highlight this phenomenon, the adsorption of charged pNIPAM-AA microgels have been performed varying the concentration of NaCl. The results are reported in Figure 10.

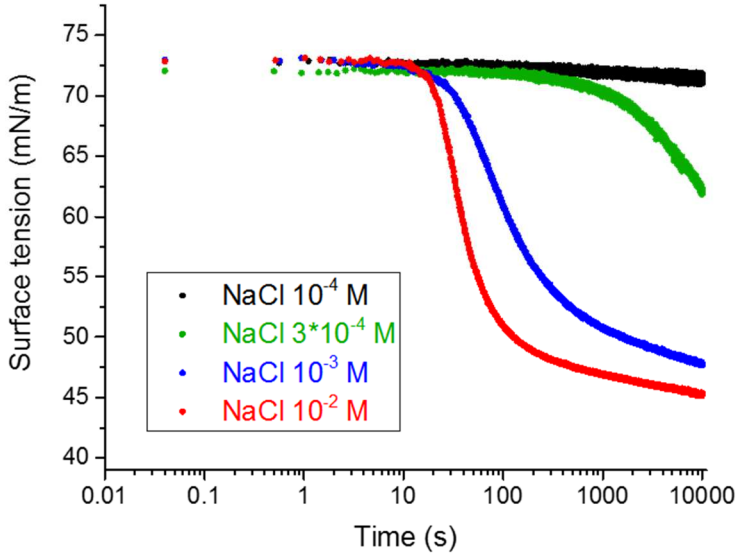

Figure 10: Progressive acceleration of pNIPAM-AA adsorption in presence of increasing amount of NaCl i.e. decreasing Debye lengths κ^{-1}. 10^{-4} M NaCl κ^{-1}=30 nm (black curve), 3 10^{-4} M NaCl κ^{-1}=17.3 nm (green curve), 10^{-3} M NaCl κ^{-1}=9.5 nm (blue curve) and 10^{-2} M NaCl κ^{-1}=3 nm (red curve).

Discussion of the microfluidic production of emulsions

As usually with a microfluidic device, the drop size is very well-calibrated, the drop size just after preparation being equal to 570 µm. The first step of the discussion is the estimation of the number of available microgels for adsorbing at the drop surface. The drop volume is ca 10^{-4} cm^3 and its surface is ca 10^6 μm^2. As the flow of the continuous phase is 4 times larger for the dispersed phase, for each drop the surrounding volume is 4 10^{-4} cm^3. For the lowest microgel concentration (0.1 wt%), the number of particles in this volume is equal to 52 10^6. It has been observed that microgels adsorbed in a compact hexagonal array (compacity=0.9) meaning that 2.7 10^6 particles are necessary to cover one drop. Microgels may adsorbed in a flatten morphology, then the number of required particles is even lower, therefore whatever the morphology the number of required particles is smaller than 2.7 10^6, which is ca 20 times smaller than the number of particles present in the continuous phase. This means that also for the microfluidic experiments there is an excess of particles. The number of particles is not a limiting parameter. Instead, from the previous results, we rather hypothesize that the critical concentration of microgels allowing drop stabilization is a consequence of the microgel concentration dependence of the adsorption kinetics. As the residence time was estimated to 1 minute, one can estimate the amount of microgels necessary to get stable emulsions using microfluidics based on the air/water interface and on the similarity with oil/water interface. Indeed, at a typical time of 60 seconds, Figure 2(a) shows that an amount of microgels comprised between 0.1 wt% and 0.5 wt% is necessary to observe a significant drop of the interfacial tension. In presence of 10^{-2} M of NaCl, the kinetics is a little accelerated and from Figure 3(a), an amount between 0.06 wt% and 0.1 wt% of microgels is required. Similarly, from Figure 5(a), an amount comprised between 0.9 wt% and 1.1 wt% of pNIPAM-AA is necessary; it decreases to between 0.1 and 0.2 wt% in presence of 10^{-2} M of NaCl. As reported in Table 3, these critical concentrations are in agreement with the critical concentrations required for drop

stabilization showing the link between adsorption kinetics and emulsification for emulsification under very low shear rates.

Table 3: Comparison between critical concentrations obtained by microfluidic and from adsorption kinetics.

Microgels	Concentration of NaCl (mol/L)	Critical concentration of microgels (wt%)	
		Microfluidic device	Adsorption kinetics
pNIPAM	10^{-4}	0.7	0.1 - 0.5
	10^{-2}	0.2	0.06 – 0.1
pNIPAM-AA	10^{-4}	1	0.9 -1.1
	10^{-2}	0.4	0.1 – 0.2

Microfluidic production of emulsion is a low-energy process. From the comparison between the centre-to-centre distance between adsorbed microgels (Fig.6c) and the non-deformed microgels in suspension, it can be deduced that microgels are not flatten at the interface, they are rather a little compressed or interpenetrated as their centre-to-centre distance represents 65% of their non-deformed hydrodynamic diameter. This microgel conformation allows avoiding bridging between neighbouring drop surfaces leading to non-flocculated drops. This result is in agreement with results reported earlier [52] where we demonstrated that bridging was strongly dependent on the drop surface coverage. Indeed surface coverage could be increased by lowering applied shear rates.

The existence of a critical amount of composite microgels has already been evoked in the literature [53] however no quantitative analysis has been reported. Note that the present phenomenon, even if the critical concentration is time-dependent, is very different from the

behaviour reported in [54] for polystyrene latex adsorption. Indeed, in their case, the authors describe the existence of a critical time that is a directly linked to the concentration of particles as a consequence of diffusion. In the present case, as shown, diffusion is not the limiting step to adsorption.

Conclusion

Using model neutral pNIPAM and charged pNIPAM-AA microgels, we evidenced the existence of a critical concentration above which microgels spontaneously and sufficiently adsorb to cause a decrease of the interfacial tension. This critical microgels concentration is higher for charged microgels. The presence of electrolyte accelerates significantly the adsorption of charged microgels and in a lower extent the adsorption of neutral microgels. When microgels adsorb, they always reach the same interfacial tension or in other words the same surface pressure. This very peculiar behaviour is very different from other systems as proteins, polyelectrolytes, star polymers, hard particles even if they share some aspects. We suggest that it is a consequence of the presence of dangling chains in the as-prepared microgels that spontaneously adsorb. The decrease of surface tension is therefore the result of hydrophobic moieties adsorption. The high affinity for the interface and the deformability of the microgels lead to an increase of the adsorbed moieties even if it means that microgels have to pack very densely at the interface. For charged microgels, electrostatics is responsible for an adsorption barrier that can be either self-screened by increasing the charged microgels concentration (endogenous ions) or screened by the presence of external ions brought for example by the presence of salt (exogenous ions). As a consequence of this critical concentration, an excess of microgels, compared to the interfacial area, is required to produce emulsions in mild conditions as with microfluidics where adsorption has to be spontaneous. This is no more the case when

high stirring is used to produce the emulsions. Indeed, in this case, much lower amounts of microgels are sufficient for forced adsorption.

ACKNOWLEDGMENTS

The authors thank the “Ministère de l’Enseignement supérieur, de la Recherche et de l’Innovation” for funding the fellowship of M.C.T.

REFERENCES

1. Pelton, R.H. and P. Chibante, *Preparation of aqueous latices with N-isopropylacrylamide.* Colloids and surfaces, 1986. **20**(3): p. 247.
2. Holden, D.A., G.R. Hendrickson, W.J. Lan, L.A. Lyon, and H.S. White, *Electrical signature of the deformation and dehydration of microgels during translocation through nanopores.* Soft Matter, 2011. **7**(18): p. 8035-8040.
3. Serpe, M.J., J. Kim, and L.A. Lyon, *Colloidal hydrogel microlenses.* Advanced Materials, 2004. **16**(2): p. 184-187.
4. Staudinger, H.H., E., *Über hochpolymere Verbindungen, 116. Mitteil.: Über das begrenzt quellbare Poly-styrol.* Berichte der deutschen chemischen Gesellschaft (A and B Series), 1935. **68**(8): p. 1618-1634.
5. Rey, M., X. Hou, J.S.J. Tang, and N. Vogel, *Interfacial arrangement and phase transitions of PNiPAm microgels with different crosslinking densities.* Soft Matter, 2017. **13**(46): p. 8717-8727.
6. Pelton, R., *Temperature-sensitive aqueous microgels.* Advances in Colloid and Interface Science, 2000. **85**(1): p. 1-33.
7. Wu, X., R.H. Pelton, A.E. Hamielec, D.R. Woods, and W. McPhee, *Kinetics of Poly(N-isopropylacrylamide) microgel latex formation.* Colloid and Polymer Science, 1994. **272**(4): p. 467.
8. Stieger, M., W. Richtering, J.S. Pedersen, and P. Lindner, *Small-angle neutron scattering study of structural changes in temperature sensitive microgel colloids.* Journal of Chemical Physics, 2004. **120**(13): p. 6197.
9. Varga, I., T. Gilanyi, R. Meszaros, G. Filipcsei, and M. Zrinyi, *Effect of cross-link density on the internal structure of poly(N-isopropylacrylamide) microgels.* Journal of Physical Chemistry B, 2001. **105**(38): p. 9071.
10. Destribats, M., V. Lapeyre, M. Wolfs, E. Sellier, F. Leal-Calderon, V. Ravaine, and V. Schmitt, *Soft microgels as Pickering emulsion stabilisers: role of particle deformability* Soft Matter, 2011. **7**: p. 7689-7698
11. Acciaro, R., T. Gilanyi, and I. Varga, *Preparation of monodisperse poly(N-isopropylacrylamide) microgel particles with homogenous cross-link density distribution.* Langmuir, 2011. **27**(12): p. 7917-7925.
12. Wei, J., Y. Li, and T. Ngai, *Tailor-made microgel particles: Synthesis and characterization.* Colloids and Surfaces A: Physicochemical and Engineering Aspects, 2016. **489**: p. 122-127.
13. Zhang, J. and R. Pelton, *Poly(N-isopropylacrylamide) at the air/water interface.* Langmuir, 1996. **12**(10): p. 2611-2612.
14. Monteux, C., C. Marliére, P. Paris, N. Pantoustier, N. Sanson, and P. Perrin, *Poly(N-isopropylacrylamide) microgels at the oil-water interface: Interfacial properties as a function of temperature.* Langmuir, 2010. **26**(17): p. 13839-13846.
15. Li, Z., W. Richtering, and T. Ngai, *Poly(N-isopropylacrylamide) microgels at the oil–water interface: temperature effect.* Soft Matter, 2014. **10**(33): p. 6182-6191.
16. Maldonado-Valderrama, J., T. del Castillo-Santaella, I. Adroher-Benítez, A. Moncho-Jordá, and A. Martín-Molina, *Thermoresponsive microgels at the air–water interface: the impact of the swelling state on interfacial conformation.* Soft Matter, 2017. **13**(1): p. 230-238.
17. Ngai, T., S.H. Behrens, and H. Auweter, *Novel emulsions stabilized by pH and temperature sensitive microgels.* Chemical Communications, 2005(3): p. 331.
18. Brugger, B. and W. Richtering, *Magnetic, thermosensitive microgels as stimuli-responsive emulsifiers allowing for remote control of separability and stability of oil in water-emulsions.* Advanced Materials, 2007. **19**(19): p. 2973.

19. Brugger, B. and W. Richtering, *Emulsions stabilized by stimuli-sensitive poly(N-isopropylacrylamide)-co- methacrylic acid polymers: Microgels versus low molecular weight polymers.* Langmuir, 2008. **24**(15): p. 7769.
20. Brugger, B., B.A. Rosen, and W. Richtering, *Microgels as stimuli-responsive stabilizers for emulsions.* Langmuir, 2008. **24**(21): p. 12202.
21. Destribats, M., V. Lapeyre, E. Sellier, F. Leal-Calderon, V. Ravaine, and V. Schmitt, *Origin and control of adhesion between emulsion drops stabilized by thermally sensitive soft colloidal particles.* Langmuir, 2012. **28**(8): p. 3744-3755.
22. Brugger, B., J. Vermant, and W. Richtering, *Interfacial layers of stimuli-responsive poly-(N-isopropylacrylamide-co- methacrylicacid) (PNIPAM-co-MAA) microgels characterized by interfacial rheology and compression isotherms.* Physical Chemistry Chemical Physics, 2010. **12**(43): p. 14573-14578.
23. Massé, P., E. Sellier, V. Schmitt, and V. Ravaine, *Impact of Electrostatics on the Adsorption of Microgels at the Interface of Pickering Emulsions.* Langmuir, 2014. **30**(49): p. 14745-14756.
24. Hoare, T. and R. Pelton, *Dimensionless plot analysis: A new way to analyze functionalized microgels.* Journal of Colloid and Interface Science, 2006. **303**(1): p. 109-116.
25. Hoare, T. and R. Pelton, *Titrametric Characterization of pH-Induced Phase Transitions in Functionalized Microgels.* Langmuir, 2006. **22**(17): p. 7342-7350.
26. Ohshima, H., *Electrophoretic Mobility of Soft Particles.* Journal of Colloid And Interface Science, 1994. **163**(2): p. 474.
27. Lele, A.K., M.M. Hirve, M.V. Badiger, and R.A. Mashelkar, *Predictions of bound water content in poly(N-isopropylacrylamide) gel.* Macromolecules, 1997. **30**(1): p. 157.
28. Busatto, C.A., H. Labie, V. Lapeyre, R. Auzely-Velty, A. Perro, N. Casis, J. Luna, D.A. Estenoz, and V. Ravaine, *Oil-in-microgel strategy for enzymatic-triggered release of hydrophobic drugs.* Journal of Colloid and Interface Science, 2017. **493**: p. 356-364.
29. Goebel, A. and K. Lunkenheimer, *Interfacial Tension of the Water/n-Alkane Interface.* Langmuir, 1997. **13**(2): p. 369-372.
30. Reculusa, S., R. Perrier-Cornet, B. Agricole, V. Heroguez, T. Buffeteau, and S. Ravaine, *Langmuir-Blodgett films of micron-sized organic and inorganic colloids.* Physical Chemistry Chemical Physics, 2007. **9**(48): p. 6385-6390.
31. Pinaud, F., K. Geisel, P. Massé, B. Cartagi, L. Isa, W. Richteing, V. Ravaine, and V. Schmitt, *Adsorption of microgels at an oil-water interface: correlation between packing and 2D elasticity.* Soft Matter (Invited) 2014 **10**: p. 6963–6974.
32. Xia, X.-f., F. Wang, and S.-f. Sui, *Effect of phospholipid on trichosanthin adsorption at the air-water interface.* Biochimica et Biophysica Acta, 2001. **1515**: p. 1-11.
33. Beverung, C.J., C.J. Radke, and H.W. Blanch, *Protein adsorption at the oil/water interface: characterization of adsorption kinetics by dynamic interfacial tension measurements.* Biophysical Chemistry, 1999. **81**(1): p. 59-80.
34. Erickson, J.S., S. Sundaram, and K.J. Stebe, *Evidence that the Induction Time in the Surface Pressure Evolution of Lysozyme Solutions Is Caused by a Surface Phase Transition.* Langmuir, 2000. **16**(11): p. 5072-5078.
35. Poirier, A., A. Banc, A. Stocco, M. In, and L. Ramos, *Multistep building of a soft plant protein film at the air-water interface.* Journal of Colloid and Interface Science, 2018. **526**: p. 337-346.
36. Miller, R., V.B. Fainerman, E.V. Aksenenko, M.E. Leser, and M.l. Miche, *Dynamic Surface Tension and Adsorption Kinetics of b-Casein at the Solution/Air Interface.* Langmuir, 2004. **20**: p. 771-777.
37. Santiago, L.G., J. Maldonado-Valderrama, A. Martín-Molina, C. Haro-Pérez, J. García-Martínez, A. Martín-Rodríguez, M.A. Cabrerizo-Vílchez, and M.J. Gálvez-Ruiz, *Adsorption of soy protein isolate at air–water and oil–water interfaces.* Colloids and Surfaces A: Physicochemical and Engineering Aspects, 2008. **323**(1): p. 155-162.

38. Destribats, M., M. Rouvet, Gehin-Delval, C. Schmitt, and B.P. Binks, *Emulsions stabilised by whey protein microgel particles: towards food-grade Pickering emulsions.* Soft Matter, 2014(10.1039/c4sm00179f).
39. Chevallier, M., A. Riaublanc, C. Lopez, P. Hamon, F. Rousseau, J. Thevenot, and T. Croguennec, *Increasing the heat stability of whey protein-rich emulsions by combining the functional role of WPM and caseins.* Food Hydrocolloids, 2018. **76**: p. 164-172.
40. Schmitt, C., C. Bovay, and M. Rouvet, *Bulk self-aggregation drives foam stabilization properties of whey protein microgels.* Food Hydrocolloids, 2014. **42**: p. 139-148.
41. Gonzalez-Jordan, A., T. Nicolai, and L. Benyahia, *Influence of the Protein Particle Morphology and Partitioning on the Behavior of Particle-Stabilized Water-in-Water Emulsions.* Langmuir, 2016. **32**(28): p. 7189-7197.
42. Rutkevičius, M., S. Allred, O.D. Velev, and K.P. Velikov, *Stabilization of oil continuous emulsions with colloidal particles from water-insoluble plant proteins.* Food Hydrocolloids, 2018. **82**: p. 89-95.
43. Silva, N.F.N., A. Saint-Jalmes, A.F. de Carvalho, and F. Gaucheron, *Development of Casein Microgels from Cross-Linking of Casein Micelles by Genipin.* Langmuir, 2014. **30**(34): p. 10167-10175.
44. Huang, Y.-R., M. Lamson, K. Matyjaszewski, and R.D. Tilton, *Enhanced interfacial activity of multi-arm poly(ethylene oxide) star polymers relative to linear poly(ethylene oxide) at fluid interfaces.* Physical Chemistry Chemical Physics, 2017. **19**(35): p. 23854-23868.
45. Noskov, B.A., A.V. Akentiev, G. Loglio, and R. Miller, *Dynamic Surface Properties of Solutions of Poly(ethylene oxide) and Polyethylene Glycols.* The Journal of Physical Chemistry B, 2000. **104**(33): p. 7923-7931.
46. Okubo, T. and K. Kobayashi, *Surface Tension of Biological Polyelectrolyte Solutions.* Journal of Colloid and Interface Science, 1998. **205**(2): p. 433-442.
47. Théodoly, O., R. Ober, and C.E. Williams, *Adsorption of hydrophobic polyelectrolytes at the air/water interface: Conformational effect and history dependence.* The European Physical Journal E, 2001. **5**(1): p. 51-58.
48. Noskov, B.A., S.N. Nuzhnov, G. Loglio, and R. Miller, *Dynamic Surface Properties of Sodium Poly(styrenesulfonate) Solutions.* Macromolecules, 2004. **37**(7): p. 2519-2526.
49. Sen, A.K., S. Roy, and V.A. Juvekar, *Effect of structure on solution and interfacial properties of sodium polystyrene sulfonate (NaPSS).* Polymer International, 2007. **56**(2): p. 167-174.
50. Yim, H., M.S. Kent, A. Matheson, M.J. Stevens, R. Ivkov, S. Satija, J. Majewski, and G.S. Smith, *Adsorption of Sodium Poly(styrenesulfonate) to the Air Surface of Water by Neutron and X-ray Reflectivity and Surface Tension Measurements: Polymer Concentration Dependence.* Macromolecules, 2002. **35**(26): p. 9737-9747.
51. Noskov, B.A., A.Y. Bilibin, A.V. Lezov, G. Loglio, S.K. Filippov, I.M. Zorin, and R. Miller, *Dynamic surface elasticity of polyelectrolyte solutions.* Colloids and Surfaces A: Physicochemical and Engineering Aspects, 2007. **298**(1): p. 115-122.
52. Destribats, M., M. Wolfs, F. Pinaud, V. Lapeyre, E. Sellier, V. Schmitt, and V. Ravaine, *Pickering Emulsions Stabilized by Soft Microgels: Influence of the Emulsification Process on Particle Interfacial Organization and Emulsion Properties.* Langmuir, 2013. **29**(40): p. 12367-12374.
53. Monteillet, H., M. Workamp, J. Appel, J.M. Kleijn, F.A.M. Leermakers, and J. Sprakel, *Ultrastrong Anchoring Yet Barrier-Free Adsorption of Composite Microgels at Liquid Interfaces.* Advanced Materials Interfaces, 2014. **1**(7): p. 1300121.
54. Yao, X., Z. Liu, M. Ma, Y. Chao, Y. Gao, and T. Kong, *Control of Particle Adsorption for Stability of Pickering Emulsions in Microfluidics.* Small, 2018. **14**(37): p. 1802902.